

Article

Circumferential and Longitudinal $\delta^{13}\text{C}$ Variability in a *Larix decidua* Trunk from the Swiss Alps

Jan Esper ^{1,*} , Dana F.C. Riechelmann ² and Steffen Holzkämper ³ ¹ Department of Geography, Johannes Gutenberg University Mainz, 55099 Mainz, Germany² Institute for Geosciences, Johannes Gutenberg University Mainz, 55099 Mainz, Germany; d.riechelmann@geo.uni-mainz.de³ Department of Physical Geography, Stockholm University, 10691 Stockholm, Sweden; steffen.holzkaemper@natgeo.su.se

* Correspondence: esper@uni-mainz.de; Tel.: +49-6131-3922296

Received: 6 December 2019; Accepted: 15 January 2020; Published: 17 January 2020



Abstract: Tree-ring stable isotopes are insightful proxies providing information on pre-instrumental climate fluctuations, yet the variability of these data within a tree trunk has not been fully explored. Here, we analyze longitudinal and circumferential changes in tree-ring $\delta^{13}\text{C}$ values from 1991–2010, considering seven height levels from 1 to 13 m above ground and six sampling directions (radii) separated by 60° around the stem. The disk samples were taken from a 360-year old European larch (*Larix decidua* Mill.) that grew at 1675 m above sea level in the Simplon Valley, Switzerland. Results show that the circumferential $\delta^{13}\text{C}$ variability, defined as the difference between the minimum and maximum isotope values within a single ring at a certain height, ranges from 0.5 to 2.8‰. These differences appear substantial as they match the range of year-to-year variations retained in long tree-ring $\delta^{13}\text{C}$ time series used for climate reconstruction. The assessment of longitudinal variability demonstrated a systematic change of $\sim 0.1\text{‰ m}^{-1}$ towards isotopically heavier (less negative) $\delta^{13}\text{C}$ values with increasing tree height, likely reflecting a vertical gradient towards isotopically heavier needle tissue due to changing microclimatic conditions and CO_2 stratification within the canopy. Calibration against regional climate data indicates no substantial signal changes in $\delta^{13}\text{C}$ values within the trunk. We conclude that the longitudinal isotope gradient adds uncertainty to long $\delta^{13}\text{C}$ chronologies derived from subfossil material of unknown (and changing) sampling heights. The large circumferential variability recorded in the sub-alpine larch suggests that more than two cores are needed to analyze absolute $\delta^{13}\text{C}$ values representative for each tree.

Keywords: stable isotopes; sampling height; tree-rings; larch tree; dendrochronology; Simplon Valley; Switzerland

1. Introduction

Tree-ring $\delta^{13}\text{C}$ is an important proxy in paleoclimate research that has been used to reconstruct temperature [1,2], precipitation [3,4], drought [5,6], and cloud cover variability [7,8] over pre-instrumental periods. Some of these reconstructions are based on $\delta^{13}\text{C}$ values from only living trees that typically cover the past one to several centuries [9–11]. Records reaching further back in time, even covering the entire past millennium, are much rarer and often combine data from living and subfossil trees [12,13]. The latter can be dead wood on the ground [8], material from logs covered in sediment [14], stems that fell into shallow lakes [7,15], and beams from historical buildings [16–20], such as the old huts and barns made of resistant *Larix decidua* boles in high elevation environments of the Swiss Alps [21].

Whereas the sampling height for dendroclimatological analyses from living trees, i.e., the height where disc or core samples are obtained, is restricted to 1–1.5 m above ground [22], this convention cannot be guaranteed for subfossil material [23]. For beams from historical buildings or wood remnants from lakes and sediments, it usually remains unknown whether a core or disc sample originates from a stem height of 1, 5, or even 10 m above ground, so that potential longitudinal $\delta^{13}\text{C}$ variability, along the tree trunk, can affect climate reconstruction uncertainty [24,25]. Similarly, $\delta^{13}\text{C}$ variability among different radii of the same level, e.g., in 1 m above ground, can affect a reconstruction if such circumferential variability is large and not mitigated by sampling several radii from different trees for stable isotope measurement (overview in [26]).

Circumferential $\delta^{13}\text{C}$ variability has been reported for various tree species and habitats (Table 1). Early work from 1980 revealed differences of up to 1.0‰ based on three decadal samples along five radii of a *Pinus ponderosa* from the United States [27], and up to 4.5‰ based on 19 annual samples along two radii of a *Quercus rubra* from the Netherlands [28]. Subsequent work demonstrated this 4.5‰ to be the upper limit of circumferential variability across species, whereas the grand mean of all studies from nine countries listed in Table 1 is 1.1‰. The range of circumferential variability also includes smaller values, down to 0.1‰, as recorded between two annually resolved $\delta^{13}\text{C}$ sequences over 73 years in a *Pinus sylvestris* from Germany [29]. The circumferential variability found in trees from various habitats prompted dendrochronologists to conclude that four cores per tree are needed to represent the absolute $\delta^{13}\text{C}$ values in tree-rings [26,30].

Table 1. Circumferential $\delta^{13}\text{C}$ variability in tree-ring studies. The first column lists the ranges of smallest to largest $\delta^{13}\text{C}$ differences among years (pentads or decades) for which radial isotope values were measured in the respective studies.

Circum. Variability	Radii	Resolution/Period	Species	Country	Source
0.5–1.0‰	5	decadal over 30 years	<i>Pinus ponderosa</i>	USA	[27]
0.1–4.5‰	2	annual over 19 years	<i>Quercus rubra</i>	Netherlands	[28]
0.5–1.0‰	4	pentadal over 130 years	<i>Phyllocladus asplen.</i>	Tasmania	[31]
0.5–2.0‰	4	annual over 100 years	<i>Picea sitchensis</i>	USA	[32]
0.5–2.5‰	4	annual over 100 years	<i>Nothofagus pumillio</i>	Chile	[32]
0.5–1.2‰	8	pentadal over 80 years	<i>Pinus edulis</i>	USA	[30]
0.5–1.3‰	3	annual over 30 years	<i>Abies pindrow</i>	India	[33]
0.1–2.3‰	2	annual over 73 years	<i>Pinus sylvestris</i>	Germany	[29]
0.5–1.0‰	3	annual over 7 years	<i>Quercus petraea</i>	N. Ireland	[34]
0.5‰	8	1 ring (1991) in 4 trees	<i>Pinus pinaster</i>	France	[35]
0.9–2.1‰	8	annual over 42 years	<i>Cryptomeria fortune</i>	China	[36]
0.4–1.6‰	8	annual over 24 years	<i>Cryptomeria fortune</i>	China	[36]
0.7–2.0‰	8	annual over 20 years	<i>Abies fabri</i>	China	[36]

Compared to the assessments of circumferential variability, studies of longitudinal $\delta^{13}\text{C}$ variability are fewer and the results less conclusive (Table 2). There are only six studies in which longitudinal variability has been analyzed over vertical distances >1 m, and only three of these studies considered trunk distances >6 m. The results range from 0.1‰ longitudinal variability, as recorded in a 25-year group over 6 m in a *Pinus sylvestris* from Sweden [37], to a maximum of 1.5‰ over a trunk distance of 2 m in a *Juniperus monosperma* from the United States based on the single tree-ring of 1981 [38]. Interestingly, there is only one early study [39] that found a small, but systematic trend (0.01‰ m⁻¹) towards isotopically heavier $\delta^{13}\text{C}$ values with increasing tree height. All other analyses revealed no systematic $\delta^{13}\text{C}$ gradient with tree height, but random variability ranging from 0.5 to 1.5‰ over vertical distances from 2 to 28 m.

Table 2. Longitudinal $\delta^{13}\text{C}$ variability in tree-ring studies. The values in the first column represent the ranges of smallest to largest average isotope composition among the different height levels being analyzed.

Longitud. Variability	Levels	Resolution	Species	Country	Source
0.01‰/m	7 levels over 14 m	7-year group	<i>Quercus robur</i>	Germany	[39]
0.05–0.1‰	3 levels over 6 m	25-year group	<i>Pinus sylvestris</i>	Sweden	[37]
1.0–1.5‰ *	5 levels over 2 m	1 year (1981)	<i>Juniperus monosp.</i>	USA	[38]
0.5–1.0‰ *	5 levels over 2.8 m	7 years (1975–1981)	<i>Pinyon pine</i>	USA	[38]
0.9‰ *	8 levels over 28 m	1 year (1983)	<i>Fagus sylvatica</i>	Germany	[40]
1‰ *	12 levels over 13 m **	1 year (1991)	<i>Pinus pinaster</i>	France	[35]

* No systematic trend along the trunk. ** Use of four 26-year old trees, including 11–14 levels over 11–14 m.

The absence of a systematic $\delta^{13}\text{C}$ gradient along the trunk is somewhat surprising, as the assessment of leaf tissue demonstrated a steep vertical gradient of 3‰ towards higher $\delta^{13}\text{C}$ values over 23 m in a *Fagus sylvatica* from Germany [40], likely triggered by changing microclimatic conditions and CO_2 stratification with tree height [41–43]. This finding was later supported in a study of 200 conifer trees from the northern Rocky Mountains, USA, revealing a vertical decrease in foliage $\delta^{13}\text{C}$ values, from the top to the bottom of the canopy, ascribed to decreasing photosynthetic capacity due to shading with increasing distances from the crown level [44]. Such a trend within the canopy has been speculated to affect the isotopic composition of tree-rings along the trunk [40], yet the relatively sparse empirical evidence available so far does not support this hypothesis.

In this paper, we present the results of ~400 stable carbon isotope measurements from a single *Larix decidua* tree from the Simplon Valley in Switzerland. Trees of this species have been used as construction timber in historical buildings, and tree-ring width (TRW) [45], maximum latewood density [46], and $\delta^{13}\text{C}$ [17] measurements of this archive have been analyzed to reconstruct climate variability over the past millennium. We assess the circumferential and longitudinal variability in tree-ring $\delta^{13}\text{C}$ values at seven trunk heights from 1 to 13 m above ground and six radii per height level. The annually resolved $\delta^{13}\text{C}$ values from 1991–2010 were calibrated against regional temperature and precipitation data to evaluate potential changes in signal strength, and the results are discussed with a focus on the paleoclimatic significance of stable carbon isotopes from tree-rings.

2. Materials and Methods

2.1. Site Description and Sample Preparation

A 20 m tall and 360-year old European larch (*Larix decidua* Mill.) at 46°10′41″ N and 08°05′11″ E in the Simplon Valley, Canton Valais, in the Swiss Alps was cut down. The tree grew in a larch-dominated forest at 1675 m a.s.l. on a 65% steep, NW-facing slope. Larch trees from this sub-alpine belt have historically been used as construction timber [21], providing the source material for millennium-length climate reconstructions based on tree-ring growth and stable isotope parameters [17,19,45,46]. European larch is a cold-tolerant tree, widely abundant and commonly cultivated in the Alps. Due to its ability to maintain stomatal conductance under non-severe dry conditions, it covers a range of sites including cold–wet to cold–dry habitats [47].

The sampling area in the Simplon Valley is characterized by well-drained podzols on silicate bedrock covered by a thin layer of organic litter and sparse ground vegetation. The felled larch was located ~400 m below the elevational treeline, at a location where the growing season, during which daily temperatures exceed 5 °C, is already relatively short, extending from May to September [48]. Data from the nearby weather station in Simplon Dorf at 1495 m a.s.l. indicate July to be the warmest month, reaching 14.5 °C and an annual mean of 5.3 °C. Precipitation sums in this elevation exceed 1300 mm and are characterized by two seasonal maxima in April–May and October.

The larch trunk was cut at 1, 3, 5, 7, 9, 11, and 13 m above ground to obtain ~5 cm thick discs representing seven height levels (Figure 1). At each level, six ~0.5 cm wide sticks were cut at

even 60° spacing around each disc representing radii A to F. We measured and crossdated the TRW at each of these 42 radii (7 discs x 6 radii) using the TSAP (Rinntech, Heidelberg, Germany) and Cofecha programs [49,50], and processed rings for the period 1991–2010 from the 360-year old larch for isotopic analysis.

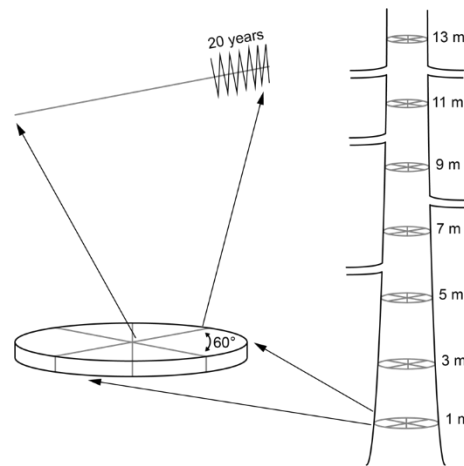


Figure 1. Schematic drawing illustrating the sampling design of a 360-year old *Larix decidua* in the Simplon Valley including seven discs in heights ranging from 1 to 13 m, six radii every 60° on each disc, and 20 tree-rings from 1991–2010 on each radius.

2.2. Stable Isotope Measurement and Analysis

For each radius, the outermost 5–7 cm were cut off, and the wood pieces leached for eight hours in distilled water and for 24 h in ethanol, all at 60 °C, to remove waxes and resins (procedure outlined in [13]). A full extraction of alpha-cellulose was not applied as the effects of this cost-intensive procedure were shown to be small [51,52]. The dried wood pieces were then fixed on a microtome, several transverse 200–300 µm thin-sections cut, and the annual rings from 1991–2010 separated using a scalpel under a reflected light binocular. The rings of five to ten of these thin-sections were typically homogenized to gain a mass of 0.5–2.5 mg sample material for each year.

The annual samples were admitted into an elemental analyzer interfaced with an IsoPrime isotope ratio mass spectrometer (GV Instruments Ltd., Manchester, UK), maintained at the Department of Inorganic and Analytical Chemistry of the Johannes Gutenberg University in Mainz, to quantify the xylem $^{13}\text{C}/^{12}\text{C}$ ratios. Results are expressed in the delta notation in parts per thousand (‰), relative to the VPDB standard for carbon isotopes. Replicated runs using IAEA-CH6 saccharose and IAEA-CH7 polyethylene standards [53] indicated the uncertainty of $\delta^{13}\text{C}$ values to be $\pm 0.1\text{‰}$.

The $\delta^{13}\text{C}$ data were corrected to account for trends from anthropogenic emissions of fossil CO_2 into the atmosphere leading to a depletion of ^{13}C in plant tissue [54]. Since additional corrections, to compensate for changes in water use efficiency [55], are currently discussed within the isotope community [10,56], we have chosen a moderate correction of 0.0073‰ per ppm CO_2 increase, as proposed in a study of juniper, pine, and oak trees from Egypt and the USA [57]. However, since all 42 radii analyzed here are equally affected by this correction, the particular procedure does not affect the comparison among radii and height levels and is of only marginal significance to the climate signal assessments.

The $\delta^{13}\text{C}$ series from 1991–2010 were compared among the six radii, A–F, by producing box plots showing the minimum and maximum differences, as well as the first, second (median), and third quartiles considering the $\delta^{13}\text{C}$ values of each single ring. We also used box plots to illustrate the range of correlations among the radii and calculated disc mean curves (DMCs) to produce time series representing the tree heights at 1, 3, 5, 7, 9, 11 and 13 m. DMCs were calculated for the original $\delta^{13}\text{C}$ and TRW measurements as well as the first-differenced versions of these data. The first-differenced

DMCs were used to estimate the climate signals at different tree heights by correlating the 1991–2010 proxy records against temperature and precipitation data from the nearby meteorological stations in Grächen and Simplon-Dorf.

3. Results and Discussion

3.1. Circumferential Variability

The assessment of radial $\delta^{13}\text{C}$ series from 1991–2010 reveals differences around the larch trunk, which vary with year. Intra-ring variability at 1 m height exceeds 2.2‰ in the early years from 1991–1993, declines in the mid-2000s, reaching a minimum of 0.68‰ in 2008, and then increases again to 2.5‰ in 2010 (Figure 2). These temporal changes in circumferential variability are characteristic for all tree heights (not shown) and include changes in radii order, i.e., radii showing lowest and highest $\delta^{13}\text{C}$ values in the 1990s (dark grey and dark green in Figure 2) are replaced by other radii in 2005 and 2009, respectively. Circumferential variability, here defined as the difference between the minimum and maximum isotope values within a single ring, is overall largest at 1 m above ground at a median of 1.8‰ (Figure 3). In addition, the range of intra-ring variability (the whiskers in Figure 3) is largest at 1 m (0.5 to 2.8‰), but both observations, median and range, do not change systematically with tree height. The smallest median circumferential variability is recorded at 7 m (0.9‰), and the smallest range between minimum and maximum differences is recorded at 9 m (1.2 to 2.1‰).

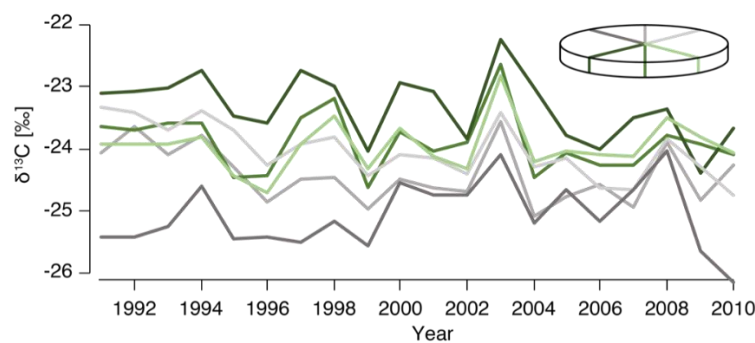


Figure 2. Circumferential $\delta^{13}\text{C}$ variability at 1 m height. Colored curves represent radii A–F.

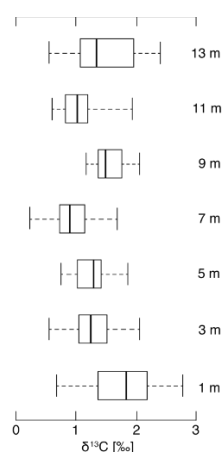


Figure 3. Circumferential $\delta^{13}\text{C}$ variability along the larch trunk. The box plots indicate the maximum and minimum values (whiskers), the lower and upper quartiles (box), and the second quartile (median) of intra-ring $\delta^{13}\text{C}$ variability among radii A–F.

The circumferential variability recorded in *Larix decidua* from the Swiss Alps is in the upper range of intra-ring $\delta^{13}\text{C}$ variability reported from other species (Table 1), except for the values observed in a *Quercus rubra* from the Netherlands that reached the highest differences at 4.5‰ [28]. The differences

among these case studies are likely controlled by variable tree species and site conditions, including elevation, slope, expositions, ground vegetation, soil, and forest composition and density. It therefore appears important to continue documenting circumferential variability in other habitats, particularly if intra-ring $\delta^{13}\text{C}$ variability is of the same magnitude as inter-ring $\delta^{13}\text{C}$ variability, as is the case here. Additionally, circumferential variability is important if samples from different radii (and trees) are pooled [38], which is often done to save costs when producing long isotope time series for the reconstruction of environmental and climatic changes over pre-instrumental periods [4,8,54]. Potential biases might arise when pooled mean chronologies integrate several radii covering different periods, and if TRW differs substantially among these radii.

The shading of needles and consequent effects on CO_2 assimilation rates have been identified as key drivers of circumferential $\delta^{13}\text{C}$ variability in stem tree rings [38,58]. These effects are likely also prevailing in our larch tree that grew in a closed-canopy forest, where competition for light is a growth-controlling and grown-shaping factor. As canopy shading effects have also been suggested to increase with grown enlargement [31,59], we might very well have emphasized these influences by considering only the outermost 20 rings of a mature, 360-year old tree. Also, the canopy architecture of our sample tree likely influenced $\delta^{13}\text{C}$ based on shading and sunlight, as the stream of photosynthates produced from leaves at the end of the tree's branches contributed to its individual circumferential variability.

Our results could additionally be influenced by considering whole-ring samples instead of only the latewood of each ring. Whereas the latter can easily be biased by the steep intra-ring $\delta^{13}\text{C}$ gradients [60], when cutting off sample material in the earlywood/latewood transition zone, the potentially varying timing of CO_2 assimilation in certain parts of the crown and effects on circumferential $\delta^{13}\text{C}$ variability [33] are likely larger in whole-ring samples integrating fractionation processes over two growing seasons [61]. Ramesh et al. [33] suggested that tracheids produced in various radii along the circumference may integrate assimilates that were produced during slightly different times of the growing season and that these time-shifts could additionally trigger circumferential $\delta^{13}\text{C}$ variability.

In addition to the absolute $\delta^{13}\text{C}$ differences, substantial variability in inter-radii correlations are recorded in the Swiss larch trunk (Figure 4). As with the absolute difference, the correlations among radii A–F do not change systematically with tree height but are smallest at 3 m (median $r = 0.31$) and largest at 7 m ($r = 0.71$). In addition, the range of correlations is quite large and includes very high values, e.g., $r = 0.97$ between two radii at 5 m, as well as significantly negative values, e.g., $r = -0.44$ between two radii at 13 m. These changes are, however, not influenced by the angular distance between radii, as we find similar results between adjacent radii as well as opposing radii (not shown).

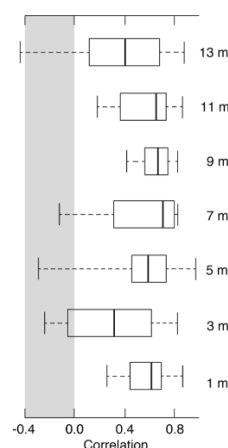


Figure 4. Inter-radii correlations at different tree heights. Box plots as in Figure 3, but for correlations among radii A–F. Value range $r < 0.0$ highlighted in grey.

Whereas the average of all inter-radii median correlations shown in Figure 4 ($r = 0.57$) demonstrates that the single radii at a certain tree height share common high-frequency variance, the large range of correlations, including negative values at four heights (3, 5, 7, 13 m), underpins the unsystematic nature of circumferential $\delta^{13}\text{C}$ variability. In the larch trunk from the Swiss Alps studied here, circumferential variability (i) is larger among certain radii but smaller among others, (ii) is larger in certain rings but smaller in others, and (iii) is larger at a certain tree height but smaller at another. These differences can partly be compensated by sampling four radii at a certain height [30], yet the pooling of radial samples not only prevents the analysis of circumferential variability but also precludes the mitigation of biases that could otherwise be achieved by detrending single stable isotope measurement series [1].

3.2. Longitudinal Variability

The comparison of DMCs reveals a systematic trend of $\sim 0.1\text{‰ m}^{-1}$ ($r^2 = 0.86$) towards isotopically heavier $\delta^{13}\text{C}$ values with increasing tree height (Figure 5). Except for the data recorded at 7 m (-23.97‰), the average carbon isotope values steadily increase from -24.13‰ at 1 m to -22.93‰ at 13 m. This trend in average values is also reflected in the DMCs over the 1991–2010 period, yet there is no single year during which the $\delta^{13}\text{C}$ are ideally ordered by tree height. This is particularly the case as the 7 m DMC (the grey curve in Figure 5) repeatedly shows lower values compared to the adjoining 5 and 3 m DMCs, and even displays the overall lowest values in 2000–2002, 2007 and 2008. Whereas the reasons for the stronger discrimination against ^{13}C in these years and the overall more depleted values at 7 m tree height remain unknown, these anomalous results effectively illustrate that conclusions can easily be biased if only two tree heights and only one or a few years are considered in assessments of longitudinal $\delta^{13}\text{C}$ variability.

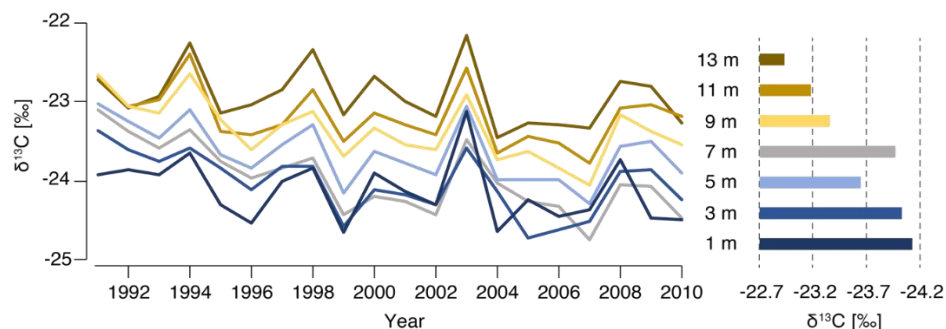


Figure 5. Longitudinal $\delta^{13}\text{C}$ variability. Left panel shows the $\delta^{13}\text{C}$ disc mean curves (DMCs), integrating the radii A–F at tree heights from 1 to 13 m. Right panel shows the average values at these heights.

The trend towards isotopically heavier values with increasing tree height found here deviates from most existing assessments conducted so far (Table 2). The reasons for this contradictory conclusion are potentially manifold, but certainly include the particular tree species—here a deciduous conifer—and study site in a high elevation alpine environment. The longitudinal $\delta^{13}\text{C}$ trend appears to be independent of TRW that shows no systematic gradient with tree height but a temporal increase from ~ 0.5 to 1.0 mm over the 1991–2010 period (Figure 6) is potentially related to regional warming and/or thinning effects. The $\delta^{13}\text{C}$ trend reported here for *Larix decidua* fits expectations based on $\delta^{13}\text{C}$ measurements of leaf tissue of a *Fagus sylvatica* from Germany, demonstrating a distinct gradient of $\sim 0.13\text{‰ m}^{-1}$ towards less negative values with increasing canopy height [40]. Our findings are also in line with gradients found in needle tissue of multiple tree species in the western United States [44], attributing these trends to shading [42,62] and water stress effects on foliar $\delta^{13}\text{C}$ [63]. Also, the effects of CO_2 stratification driven by the decomposition of soil organic matter [41,64] could contribute to the longitudinal trend recorded here.

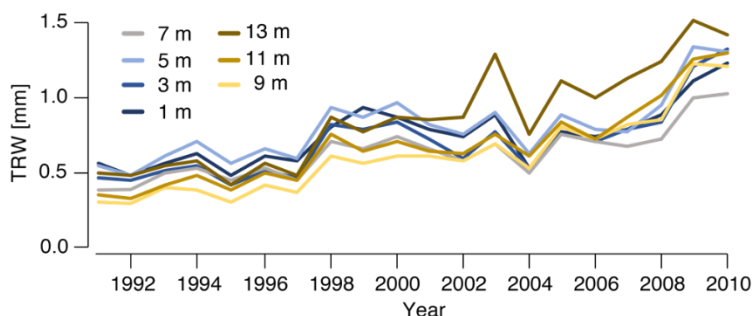


Figure 6. Longitudinal TRW variability. TRW disc mean curves (DMCs) at tree heights from 1 to 13 m.

Our results might also differ from previous findings because we sampled several radii and measured six sequences of 20 rings in each level along the trunk. Averaging the radial series to form DMCs compensates for circumferential variability that would otherwise affect the results, if only one radius and only one ring or group of rings were considered. This conclusion is underpinned by the early work of Tans and Mook (1980) [28], who demonstrated substantial longitudinal $\delta^{13}\text{C}$ variability of 0.8‰ over only 40 cm in a *Quercus rubra* L. from the Netherlands. Yet this variability diminished to only 0.2‰ 40cm^{-1} if the fiber orientation within the oak stem was considered. These results show that each fiber has its own $\delta^{13}\text{C}$ identity, and that sampling several radii per height level, and averaging these supports discerning longitudinal trends over longer stem distances. Further studies of annually resolved $\delta^{13}\text{C}$ series (i) over two or more decades, (ii) along 4–8 radii, (iii) at multiple heights, (iv) over 10+ meters are needed to test whether the longitudinal gradient recorded here in *Larix decidua* from the Swiss Alps can be validated for other tree species and habitats.

3.3. Climate Signals

Despite the large circumferential and longitudinal variabilities recorded in our larch trunk, the $\delta^{13}\text{C}$ DMCs displayed in Figure 5 correlate at $r_{1992-2010} = 0.82$, revealing substantial covariance among tree heights. The corresponding seven TRW DMCs even correlate at $r_{1992-2010} = 0.94$, but this coefficient is inflated by a common trend towards wider rings (Figure 6). Removal of the long-term trends from the $\delta^{13}\text{C}$ and TRW data, by first differencing the DMCs (Figure 7), demonstrates that significant high-frequency co-variability is retained in both tree-ring parameters along the trunk ($r_{\delta^{13}\text{C}} = 0.86$, $r_{\text{TRW}} = 0.88$). As the mean $\delta^{13}\text{C}$ and TRW time series (red curves in Figure 7) also correlate significantly at $r_{1992-2010} = 0.54$, this shared variability indicates that both proxies are controlled by similar climatic drivers.

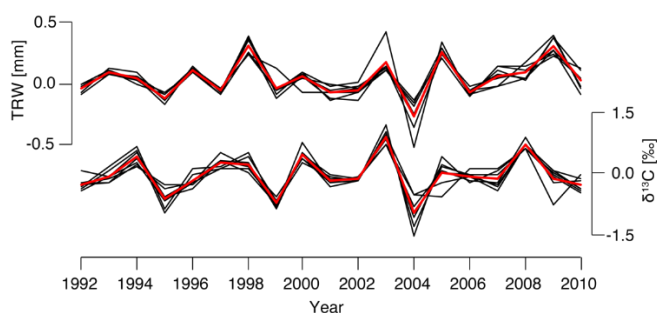


Figure 7. High frequency TRW and $\delta^{13}\text{C}$ variability. Top panel shows first-differenced TRW disc mean curves (DMCs) at seven tree heights (black) together with their arithmetic mean (red). Bottom panel shows the first-differenced $\delta^{13}\text{C}$ DMCs and mean.

Calibration against monthly climate data shows that the highest correlations are recorded with regional May–August temperatures ($\delta^{13}\text{C}$ and TRW) and previous-year May–August precipitation ($\delta^{13}\text{C}$) (Figure 8). The latter signal seems to be a side effect of our approach of considering whole-ring

samples that include earlywood material from stored photosynthates, which are additionally affected by previous-year hydroclimatic conditions [65]. The dominant, current-year warm season temperature signal is stronger and longitudinally more balanced in $\delta^{13}\text{C}$ compared to TRW. Whereas the $\delta^{13}\text{C}$ correlations range from $r = 0.57$ at 3 m to $r = 0.79$ at 13 m, the TRW results are consistently lower ($r = 0.48$ – 0.60) except for the deviating coefficient obtained for the 13 m DMC ($r_{13\text{m}} = 0.78$). However, given the short calibration period that includes only 20 years from 1992–2010, all longitudinal differences shown in Figure 8a are insignificant, and therefore do not support specific considerations of certain tree heights to potentially increase signal strength in tree-ring $\delta^{13}\text{C}$ (or TRW) time series.

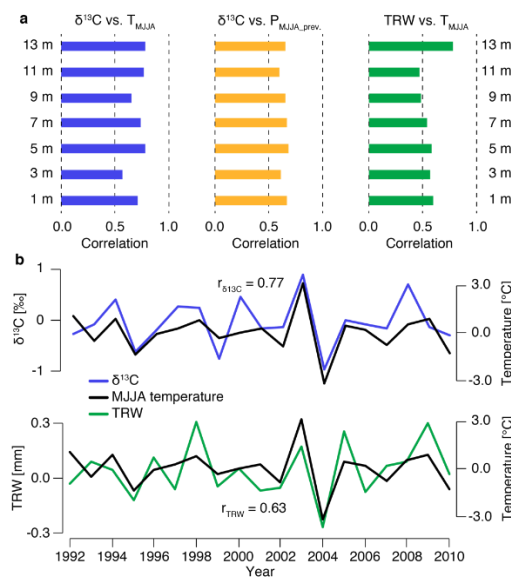


Figure 8. High frequency climate signals. (a) Pearson correlations $\delta^{13}\text{C}$ disc mean curves (DCMs) against May–August (MJJA) mean temperatures (blue), $\delta^{13}\text{C}$ DCMs against previous-year MJJA precipitation (yellow), and TRW DCMs against MJJA temperatures. Both the proxy and instrumental data were first-differenced. Correlations calculated over 1992–2010. (b) The $\delta^{13}\text{C}$ mean tree curve (MTC) in blue and the TRW MTC in green plotted together with MJJA temperatures (black) from 1992–2010.

The high covariance among first-differenced DMCs also controls the calibration of the $\delta^{13}\text{C}$ and TRW mean tree curves against May–August temperatures (Figure 8b). Again, the coefficient is slightly higher for $\delta^{13}\text{C}$ compared to TRW, but the difference is statistically insignificant. On the other hand, the correlation values are surprisingly high (particularly the $r_{\delta^{13}\text{C}} = 0.77$), considering that only one tree is compared against regional climate data. These findings reinforce the climate sensitivity of tree ring carbon isotopes and the skill of such data to particularly reconstruct high-frequency temperature variations over longer timescales [66,67].

4. Conclusions

By analyzing 42 annually resolved $\delta^{13}\text{C}$ time series spanning the 1991–2010 period, at seven height levels, we found substantial circumferential and longitudinal $\delta^{13}\text{C}$ variability within a single *Larix decidua* trunk from a sub-alpine environment in the Swiss Alps. Circumferential variability is comparable among different tree heights, and the range of values (0.5–2.8‰ at 1 m) is near the upper limit reported from other species and habitats. The variability along the trunk is of similar magnitude (1.2‰ over 12 m), yet we, for the first time, demonstrate a systematic trend of 0.1‰ m^{-1} towards isotopically heavier values with increasing tree height. This trend is in line with expectations based on $\delta^{13}\text{C}$ measurements of leaf tissue within a *Fagus sylvatica* treetop [40], which showed a vertical gradient of 0.13‰ m^{-1} towards less negative $\delta^{13}\text{C}$ with height, likely driven by CO_2 stratification and changing microclimatic conditions.

Both the circumferential and longitudinal variabilities are of practical importance as they are of the same magnitude as the inter-annual $\delta^{13}\text{C}$ variability that is typically used to reconstruct environmental and climatic changes over longer timescales. Whereas some of the intra-ring variability recorded at a certain stem height (e.g., breast height) can be compensated by averaging samples from several radii, the systematic longitudinal gradient reported here appears to be a fundamental concern of long-term climate reconstructions from $\delta^{13}\text{C}$. If discs and cores are obtained at unknown sampling heights, which is typically the case in composite chronologies including samples from historical buildings, lakes, and sediments, longitudinal variability can add substantial uncertainty to reconstructions from such compilations. It is therefore recommended to assess offsets between single $\delta^{13}\text{C}$ series, and apply dendrochronological detrending techniques to mitigate potential biases on the low-frequency spectrum of long stable carbon isotope chronologies. The high-frequency, inter-annual signal, which in our larch tree from the Swiss Alps is controlled by May–August temperatures, remains largely unaffected by the circumferential and longitudinal variabilities reported here.

Author Contributions: J.E. and S.H. designed the study and wrote the manuscript with input from D.F.C.R. and S.H. supported the measurement campaign, D.F.C.R. conducted the field work, and J.E. and S.H. performed the analyses. All authors have read and agreed to the published version of the manuscript.

Funding: Supported by German Science Foundation projects ES 161/9-1 and HA 8048/1-1.

Acknowledgments: We thank Frank Cimander, Daniel Nievergelt, Markus Kochbeck, Willi Dindorf, and members of forestry district in Simplon for field and technical support.

Conflicts of Interest: The authors declare no conflict of interest.

References

- Esper, J.; Konter, O.; Krusic, P.; Saurer, M.; Holzkämper, S.; Büntgen, U. Long-term summer temperature variations in the Pyrenees from detrended stable carbon isotopes. *Geochronometria* **2015**, *42*, 53–59. [[CrossRef](#)]
- Szymczak, S.; Joachimski, M.M.; Bräuning, A.; Hetzer, T.; Kuhlemann, J. A 560yr summer temperature reconstruction for the Western Mediterranean basin based on stable carbon isotopes from *Pinus nigra* ssp. *laricio* (Corsica/ France). *Clim. Past* **2012**, *8*, 1737–1749. [[CrossRef](#)]
- Holzkämper, S.; Kuhry, P.; Kultti, S.; Gunnarson, B.E.; Sonninen, E. Stable isotopes in tree rings as proxies for winter precipitation changes in the Russian Arctic over the past 150 years. *Geochronometria* **2008**, *32*, 37–46. [[CrossRef](#)]
- Treydte, K.; Schleser, G.H.; Helle, G.; Frank, D.C.; Winiger, M.; Haug, G.H.; Esper, J. The twentieth century was the wettest period in Northern Pakistan over the past millennium. *Nature* **2006**, *440*, 1179–1182. [[CrossRef](#)] [[PubMed](#)]
- Kress, A.; Saurer, M.; Siegwolf, R.T.W.; Frank, D.C.; Esper, J.; Bugmann, H. A 350 year drought reconstruction from Alpine tree ring stable isotopes. *Glob. Biogeochem. Cycl.* **2010**, *24*, 2. [[CrossRef](#)]
- Leavitt, S.W.; Chase, T.N.; Rajagopalan, B.; Lee, E.; Lawrence, P.J.; Woodhouse, C.A. Southwestern US drought maps from pinyon tree-ring carbon isotopes. *Eos Trans.* **2007**, *88*, 39–40. [[CrossRef](#)]
- Helama, S.; Arppe, L.; Timonen, M.; Mielikäinen, K.; Oinonen, M. A 7.5 ka chronology of stable carbon isotopes from tree rings with implications for their use in palaeo-cloud reconstruction. *Glob. Planet. Chang.* **2018**, *170*, 20–33. [[CrossRef](#)]
- Loader, N.J.; Young, G.H.F.; Grudd, H.; McCarroll, D. Stable carbon isotopes from Torneträsk, northern Sweden provide a millennial length reconstruction of summer sunshine and its relationship to Arctic circulation. *Quat. Sci. Rev.* **2013**, *62*, 97–113. [[CrossRef](#)]
- Esper, J.; Holzkämper, S.; Büntgen, U.; Schöne, B.; Keppler, F.; Hartl, C.; St. George, S.; Riechelmann, D.F.C.; Treydte, K. Site-specific climatic signals in stable isotope records from Swedish pine forests. *Trees* **2018**, *32*, 855–869. [[CrossRef](#)]
- Konter, O.; Holzkämper, S.; Helle, G.; Büntgen, U.; Saurer, M.; Esper, J. Climate sensitivity and parameter coherency in annually resolved $\delta^{13}\text{C}$ and $\delta^{18}\text{O}$ from *Pinus uncinata* tree-ring data in the Spanish Pyrenees. *Chem. Geol.* **2014**, *377*, 12–19. [[CrossRef](#)]
- Tardif, J.C.; Conciatori, F.; Leavitt, S.W. Tree rings, $\delta^{13}\text{C}$ and climate in *Picea glauca* growing near Churchill, subarctic Manitoba, Canada. *Chem. Geol.* **2008**, *252*, 88–101. [[CrossRef](#)]

12. Kłusek, M.; Grabner, M.; Pawełczyk, S.; Pawlyta, J. An 1800-year stable carbon isotope chronology based on sub-fossil wood from Lake Schwarzensee, Austria. *Palaeogeogr. Palaeoclimatol. Palaeoecol.* **2019**, *514*, 65–76. [[CrossRef](#)] [[PubMed](#)]
13. Sidorova, O.V.; Siegwolf, R.; Saurer, M.; Naurzbaev, M.M.; Vaganov, E.A. Isotopic composition ($\delta^{13}\text{C}$, $\delta^{18}\text{O}$) in wood and cellulose of Siberian larch trees for early medieval and recent periods. *J. Geophys. Res.* **2008**, *113*, G2. [[CrossRef](#)]
14. Sass-Klaassen, U.; Poole, I.; Wils, T.; Helle, G.; Schleser, G.H.; van Bergen, P.F. Carbon and oxygen isotope dendrochronology in sub-fossil bog oak tree rings—A preliminary study. *IAWA J.* **2005**, *26*, 121–136. [[CrossRef](#)]
15. Kłusek, M.; Pawełczyk, S. Stable carbon isotope analysis of subfossil wood from Austrian Alps. *Geochronometria* **2014**, *41*, 400–408. [[CrossRef](#)]
16. Etien, N.; Daux, V.; Masson-Delmotte, V.; Stievenard, M.; Bernard, V.; Durost, S.; Guillemin, M.T.; Mestre, O.; Pierre, M. A bi-proxy reconstruction of Fontainebleau (France) growing season temperature from A.D. 1596 to 2000. *Clim. Past* **2008**, *4*, 1–16. [[CrossRef](#)]
17. Hangartner, S.; Kress, A.; Saurer, M.; Frank, D.; Leuenberger, M. Methods to merge overlapping tree-ring isotope series to generate multi-centennial chronologies. *Chem. Geol.* **2012**, *294*, 127–134. [[CrossRef](#)]
18. Haupt, M.; Weigl, M.; Grabner, M.; Boettger, T. A 400-year reconstruction of July relative air humidity for the Vienna region (eastern Austria) based on carbon and oxygen stable isotope ratios in tree-ring latewood cellulose of oaks (*Quercus petraea* Matt. Liebl.). *Clim. Chang.* **2011**, *105*, 243–262. [[CrossRef](#)]
19. Kress, A.; Hangartner, S.; Bugmann, H.; Büntgen, U.; Frank, D.C.; Leuenberger, M.; Siegwolf, R.T.W.; Saurer, M. Swiss tree rings reveal warm and wet summers during medieval times. *Geophys. Res. Lett.* **2014**, *41*, 1732–1737. [[CrossRef](#)]
20. Masson-Delmotte, V.; Raffalli-Delerce, G.; Danis, P.A.; Yiou, P.; Stievenard, M.; Guibal, F.; Jouzel, J.; Mestre, O.; Bernard, V.; Goosse, H.; et al. Changes in European precipitation seasonality and in drought frequencies revealed by a four-century-long tree-ring isotopic record from Brittany, western France. *Clim. Dyn.* **2005**, *24*, 57–69. [[CrossRef](#)]
21. Büntgen, U.; Bellwald, I.; Kalbermatten, H.; Schmidhalter, M.; Frank, D.C.; Freund, H.; Bellwald, W.; Neuwirth, B.; Nüsser, M.; Esper, J. 700 years of settlement and building history in the Lötschental, Switzerland. *Erdkunde* **2006**, *60*, 96–112. [[CrossRef](#)]
22. Fritts, H.C. *Tree Rings and Climate*; Academic Press: London, UK, 1976.
23. Tegel, W.; Vanmoerkerke, J.; Büntgen, U. Updating historical tree-ring records for climate reconstruction. *Quat. Sci. Rev.* **2010**, *29*, 1957–1959. [[CrossRef](#)]
24. Esper, J.; Frank, D.C.; Battipaglia, G.; Büntgen, U.; Holert, C.; Treydte, K.; Siegwolf, R.; Saurer, M. Low-frequency noise in $\delta^{13}\text{C}$ and $\delta^{18}\text{O}$ tree ring data: A case study of *Pinus uncinata* in the Spanish Pyrenees. *Glob. Biogeochem. Cycl.* **2010**, *24*, 4. [[CrossRef](#)]
25. Helama, S.; Arppe, L.; Timonen, M.; Mielikäinen, K.; Oinonen, M. Age-related trends in subfossil tree-ring $\delta^{13}\text{C}$ data. *Chem. Geol.* **2015**, *416*, 28–35. [[CrossRef](#)]
26. Leavitt, S.W. Tree-ring C–H–O isotope variability and sampling. *Sci. Total Environ.* **2010**, *408*, 5244–5253. [[CrossRef](#)] [[PubMed](#)]
27. Mazany, T.; Lerman, J.C.; Long, A. Carbon-13 in tree-ring cellulose as an indicator of past climates. *Nature* **1980**, *287*, 432–435. [[CrossRef](#)]
28. Tans, P.P.; Mook, W.G. Past atmospheric CO₂ levels and the $^{13}\text{C}/^{12}\text{C}$ ratios in tree rings. *Tellus* **1980**, *32*, 268–283. [[CrossRef](#)]
29. Hemmann, A.G. Umweltrelevanz von $\delta^{13}\text{C}$ Korrelationen an Jahrringen Rezenter Kiefern (*Pinus Sylvestris*). Ph.D. Thesis, University of Cologne, Cologne, Germany, 1993.
30. Leavitt, S.W.; Long, A. Sampling strategy for stable carbon isotope analysis of tree rings in pine. *Nature* **1984**, *311*, 145–147. [[CrossRef](#)]
31. Francey, R.J. Tasmanian tree rings belie suggested anthropogenic $^{13}\text{C}/^{12}\text{C}$ trends. *Nature* **1981**, *290*, 232–235. [[CrossRef](#)]
32. Stuiver, M.; Braziunas, T.F. Tree cellulose $^{13}\text{C}/^{12}\text{C}$ isotope ratios and climate change. *Nature* **1987**, *328*, 58–60. [[CrossRef](#)]
33. Ramesh, R.; Bhattacharya, S.K.; Gopalan, K. Dendrochronological implications of isotope coherence in trees from Kashmir Valley, India. *Nature* **1985**, *317*, 802–804. [[CrossRef](#)]

34. Robertson, I.; Field, E.M.; Heaton, T.H.E.; Pilcher, J.R.; Pollard, M.; Switsur, R.; Waterhouse, J.S. Isotope coherence in oak cellulose. In *Problems of Stable Isotopes in Tree-Rings, Lake Sediments and Peat-Bogs as Climatic Evidence for the Holocene*; Frenzel, B., Stauffer, B., Weib, M.M., Eds.; G. Fischer: Stuttgart, Germany, 1995; pp. 141–155.
35. Nguyen-Queyrens, A.; Ferhi, A.; Loustau, D.; Guehl, J.M. Within-ring $\delta^{13}\text{C}$ spatial variability and interannual variations in wood cellulose of two contrasting provenances of *Pinus pinaster*. *Can. J. For. Res.* **1998**, *28*, 766–773. [[CrossRef](#)]
36. Chen, B.; Qian, J.; Pu, P.; Wang, G.; Tu, Q. Azimuthal distribution of stable carbon isotopes in tree rings and its application in climate reconstructions. *J. Nanjing Inst. Meteorol.* **2002**, *25*, 463–471. (In Chinese)
37. De Silva, M.P. $\delta^{13}\text{C}$ -Variationen in Baumjahresringen als Folge des Anthropogenen CO_2 -Anstiegs der Atmosphäre: Untersuchung des Einflusses von Klimaparametern. Ph.D. Thesis, Rheinisch-Westfälische Hochschule, Aachen, Germany, 1978.
38. Leavitt, S.W.; Long, A. Stable-carbon isotope variability in tree foliage and wood. *Ecology* **1986**, *67*, 1002–1010. [[CrossRef](#)]
39. Freyer, H.D.; Wiesberg, L. Anthropogenic carbon-13 decrease in atmospheric carbon dioxide as recorded in modern wood. In *FAO/IAEA Symposium on Isotope Ratios as Pollutant Source and Behavior Indicators*; International Atomic Energy Association: Vienna, Austria, 1975; pp. 49–62.
40. Schleser, G.H. $\delta^{13}\text{C}$ pattern in a forest tree as an indicator of carbon transfer in trees. *Ecology* **1992**, *73*, 1922–1925. [[CrossRef](#)]
41. Vogel, J.C. Recycling of carbon in a forest environment. *Oecologia Plant* **1978**, *13*, 89–94.
42. Francey, R.J.; Gifford, R.M.; Sharkey, T.D.; Weir, B. Physiological influences on carbon isotope discrimination in huon pine (*Lagarostrobos franklinii*). *Oecologia* **1985**, *66*, 211–218. [[CrossRef](#)]
43. Ehleringer, J.R.; Field, C.B.; Lin, Z.F.; Kuo, C.Y. Leaf carbon isotope and mineral composition in subtropical plants along an irradiance cline. *Oecologia* **1986**, *70*, 520–526. [[CrossRef](#)]
44. Duursma, R.A.; Marshall, J.D. Vertical canopy gradients in $\delta^{13}\text{C}$ correspond with leaf nitrogen content in a mixed-species conifer forest. *Trees* **2006**, *20*, 496–506. [[CrossRef](#)]
45. Büntgen, U.; Esper, J.; Frank, D.C.; Nicolussi, K.; Schmidhalter, M. A 1052-year tree-ring proxy for Alpine summer temperatures. *Clim. Dyn.* **2005**, *25*, 141–153. [[CrossRef](#)]
46. Büntgen, U.; Frank, D.C.; Nievergelt, D.; Esper, J. Summer temperature variations in the European Alps, A.D. 755–2004. *J. Clim.* **2006**, *19*, 5606–5623. [[CrossRef](#)]
47. Badalotti, A.; Anfodillo, T.; Grace, J. Evidence of osmoregulation in *Larix decidua* at Alpine treeline and comparative responses to water availability of two co-occurring evergreen species. *Ann. For. Sci.* **2000**, *57*, 623–633. [[CrossRef](#)]
48. Moser, L.; Fonti, P.; Büntgen, U.; Esper, J.; Luterbacher, J.; Franzen, J.; Frank, D. Timing and duration of European larch growing season along altitudinal gradients in the Swiss Alps. *Tree Phys.* **2009**, *30*, 225–233. [[CrossRef](#)] [[PubMed](#)]
49. Holmes, R.L. Computer-assisted quality control in tree-ring dating and measurement. *Tree Ring Bull.* **1983**, *43*, 69–78.
50. Rinn, F. *TSAP-Win Professional*; Rinntech: Heidelberg, Germany, 2007.
51. Cullen, L.E.; Grierson, P.F. Is cellulose extraction necessary for developing stable carbon and oxygen isotopes chronologies from *Callitris glaucophylla*? *Palaeogeogr. Palaeoclimatol. Palaeoecol.* **2006**, *236*, 206–216. [[CrossRef](#)]
52. Riechelmann, D.F.C.; Maus, M.; Dindorf, W.; Konter, O.; Schöne, B.R.; Esper, J. Comparison of $\delta^{13}\text{C}$ and $\delta^{18}\text{O}$ from cellulose, whole wood, and resin-free whole wood from an old high elevation *Pinus uncinata* in the Spanish central Pyrenees. *Isot. Environ. Health Stud.* **2016**, *52*, 694–705. [[CrossRef](#)]
53. Knöller, K.; Boettger, T.; Weise, S.M.; Gehre, M. Carbon isotope analyses of cellulose using two different on-line techniques (elemental analysis and high-temperature pyrolysis)—A comparison. *Rap. Commun. Mass Spectrom.* **2005**, *19*, 343–348. [[CrossRef](#)]
54. Treydte, K.S.; Frank, D.C.; Saurer, M.; Helle, G.; Schleser, G.H.; Esper, J. Impact of climate and CO_2 on a millennium-long tree-ring carbon isotope record. *Geochim. Cosmochim. Acta* **2009**, *73*, 4635–4647. [[CrossRef](#)]
55. Frank, D.C.; Poulter, B.; Saurer, M.; Esper, J.; Huntingford, C.; Helle, G.; Treydte, K.; Zimmermann, N.E.; Schleser, G.H.; Ciais, P.; et al. Water-use efficiency and transpiration across European forests during the Anthropocene. *Nature Clim. Chang.* **2015**, *5*, 579–583. [[CrossRef](#)]

56. Schubert, B.A.; Jahren, A.H. The effect of atmospheric CO₂ concentration on carbon isotope fractionation in C₃ land plants. *Geochim. Cosmochim. Acta* **2012**, *96*, 29–43. [[CrossRef](#)]
57. Kürschner, K. *Leaf Stomata as Biosensors of Paleoatmospheric CO₂ Levels*; LPP Contribution Series 5: Utrecht, The Netherlands, 1996.
58. Francey, R.J. Carbon isotope measurements in baseline air, forest canopy air, and plants. In *The Changing Carbon Cycle*; Trabalka, J.R., Reichle, D.E., Eds.; Springer: New York, NY, USA, 1986; pp. 160–174.
59. Freyer, H.D.; Belacy, N. ¹³C/¹²C records in northern hemispheric trees during the past 500 years—Anthropogenic impact and climatic superpositions. *J. Geophys. Res. Oceans* **1986**, *88*, 6844–6852. [[CrossRef](#)]
60. Helle, G.; Schleser, G.H. Beyond CO₂-fixation by Rubisco—An interpretation of ¹³C/¹²C variations in tree rings from novel intra-seasonal studies on broad-leaf trees. *Plant Cell Environ.* **2004**, *27*, 367–380. [[CrossRef](#)]
61. Switsur, V.R.; Waterhouse, J.S.; Field, E.M.; Carter, A.H.C.; Loader, N.J. Stable isotope studies in tree rings from oak—Techniques and some preliminary results. *Paläoklimaforschung* **1995**, *15*, 129–140.
62. Farquhar, G.D.; Ehleringer, J.R.; Hubick, K.T. Carbon isotope discrimination and photosynthesis. *Annu. Rev. Plant Physiol. Plant Mol. Biol.* **1989**, *40*, 503–537. [[CrossRef](#)]
63. Koch, G.W.; Sillett, S.C.; Jennings, G.M.; Davis, S.D. The limits to tree height. *Nature* **2004**, *428*, 851–854. [[CrossRef](#)]
64. Palonen, V.; Pumpanen, J.; Kulmala, L.; Levin, I.; Heinonsalo, J.; Vesala, T. Seasonal and diurnal variations in atmospheric and soil air ¹⁴CO₂ in a boreal scots pine forest. *Radiocarbon* **2018**, *60*, 283–297. [[CrossRef](#)]
65. Kagawa, A.; Sugimoto, A.; Maximov, T.C. Seasonal course of translocation, storage and remobilization of ¹³C pulse-labeled photoassimilate in naturally growing *Larix gmelinii* saplings. *New Phytol.* **2006**, *171*, 793–803. [[CrossRef](#)]
66. Hafner, P.; Robertson, I.; McCarroll, D.; Loader, N.J.; Gagen, M.; Bale, R.J.; Jungner, H.; Sonninen, E.; Hiltavuori, E.; Levanič, T. Climate signals in the ring widths and stable carbon, hydrogen and oxygen isotopic composition of *Larix decidua* growing at the forest limit in the southeastern European Alps. *Trees* **2011**, *25*, 1141–1154. [[CrossRef](#)]
67. Treydte, K.; Frank, D.; Esper, J.; Andreu, L.; Bednarz, Z.; Berninger, F.; Boettger, T.; Filot, M.; Grabner, M.; Grabner, M.; et al. Signal strength and climate calibration of a European tree-ring isotope network. *Geophys. Res. Lett.* **2007**, *34*, 24. [[CrossRef](#)]



© 2020 by the authors. Licensee MDPI, Basel, Switzerland. This article is an open access article distributed under the terms and conditions of the Creative Commons Attribution (CC BY) license (<http://creativecommons.org/licenses/by/4.0/>).